Extended Abstracts of the 2016 International Conference on Solid State Devices and Materials, Tsukuba, 2016, pp439-440

J-3-03

Field effect transistor of thin anatase obtained through solid-state transformation of $Ti_{0.87}O_2$ nanosheet

[1*]S. Sekizaki, [2]M. Osada, & [1,3]K. Nagashio
[1]The University of Tokyo, 7-3-1 Hongo, Bunkyo-ku, Tokyo, 113-8656 Japan
[2]NIMS, 1-1 Namiki, Tsukuba, Ibaraki, 305-0044 Japan
[3]PRESTO-JST, Japan
[*]E-mail: sekizaki@ncd.t.u-tokyo.ac.jp

$Ti_{0.87}O_2$ nanosheet is 2 dimensional oxide insulator with the monolayer thickness of 0.7 nm. In this work, we demonstrate the transistor operation of anatase FETs with the channel thickness thinner than 10 nm through the solid state transformation from $Ti_{0.87}O_2$ nanosheet.

1. Introduction

TiO_2 is the most conventional photocatalytic material. The ultraviolet (UV) irradiation excites *e-h* pairs, which oxidize organic matter on TiO_2. If carrier generation by the UV irradiation is replaced to that by electric field effect, the application of TiO_2 expands widely. Although the backgate TiO_2 field effect transistors (FETs) have been reported so far (**Table 1**), it is difficult to induce carriers on TiO_2 surface by electric field effect because the thickness of TiO_2 layer is generally thicker than 20nm in order to retain the crystal quality.

Here, $Ti_{0.87}O_2$ nanosheet is the 2-dimensional nanosheet with 0.7-nm thickness, which is obtained by soft chemical reaction of layered $K_{0.8}Ti_{1.73}Li_{0.27}O_4$ single crystal (**Fig. 1**) [4]. $Ti_{0.87}O_2$ nanosheet is insulator with quite high resistivity because the original layered structure is retained by introducing 13% Ti vacancies. Moreover, it transforms into anatase and rutile with increasing the annealing temperature. Therefore, if the anatase TiO_2 FETs with the thickness thinner than 10 nm can be fabricated through the solid state transformation from $Ti_{0.87}O_2$ nanosheet, the large amount of carriers may be induced on the surface. In this study, we focus on the fabrication of anatase thin film FETs and discuss FET characteristics.

2. Demonstration of anatase TiO_2 FET

$Ti_{0.87}O_2$/tetrabutylammonium suspension was spin-coated on SiO_2 (90 nm)/n^+-Si substrate at 3000 rpm, and annealed at 800 °C in air for 1 h. **Figure 2** shows an optical microscope image with nomarski for the sample after the annealing. TiO_2 nanosheets are classified into three types, monolayer, multilayers (laminated during the spin-coating), and bulk (not exfoliated), based on the crystal morphology. These classification is confirmed by the Raman analysis, as shown in **Fig. 3(a)**. The main peak of anatase, $E_g(1)$, is

Table.1 FET characteristics.

	Phase	Method	Thickness(nm)	$I_{on/off}$	μ(cm^2/Vs)
present	anatase	2D Phase transition	8∼15	10^6	0.23
Ref. [1]	anatase	PLD	20	10^5	10
Ref. [2]	rutile	Single crystal	NA	10^4	0.1
Ref. [3]	amorphous	PE-ALD	30	10^8	0.08

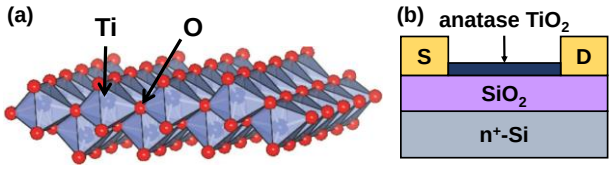

Fig. 1 (a) The crystal structure of $Ti_{0.87}O_2$ nanosheet. [4] (b) Schematic of back gate TiO_2 FET.

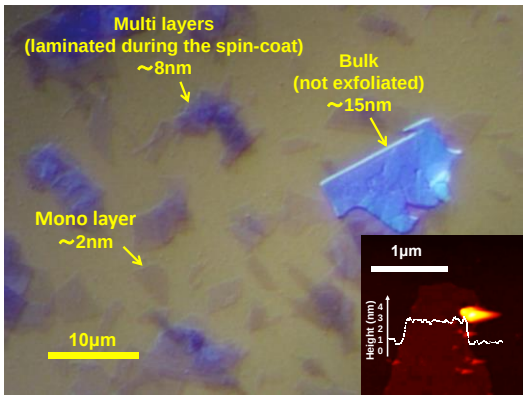

Fig. 2 Optical microscope image with nomarski for the sample after the annealing. Insert: AFM image of monolayer.

observed at 142 cm^{-1} for multilayer and bulk, but not for monolayer. Furthermore, the intensity of $B_{1g}(1)$ for bulk is higher than that for multilayer, suggesting that the crystallinity of anatase can be reliably evaluated by $B_{1g}(1)$. It seems that monolayer nanosheet become amorphous, probably because at least two layers of nanosheets are required to satisfy the periodicity of anatase crystal structure. **Figure 3(b)** shows the Intensity ratio of $E_g(1)$ and Si peak at 300 cm^{-1} as a function of annealing temperature for multilayer nanosheets. The highest intensity ratio, which indicates the highest crystallinity, is found at 800 °C. Therefore, the annealing temperature of 800 °C is selected for subsequent characterizations. The crystallinity was analyzed more in detail by electron backscattering diffraction pattern (EBSP). The bulk sample shows the clear single crystalline nature, while multilayer and

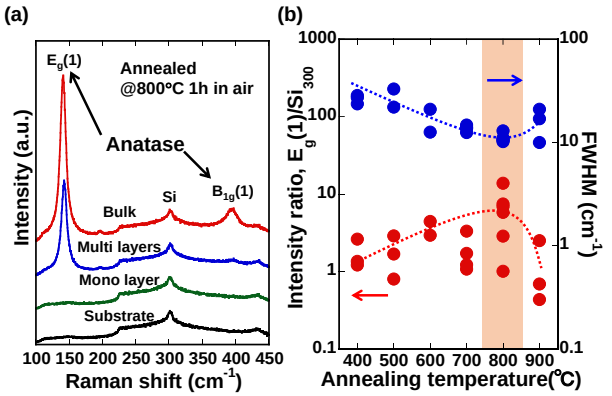

Fig. 3 (a) Raman Spectra for all types of anatase. (b) Intensity ratio for $E_g(1)/Si_{300}$ and FWHM of $E_g(1)$ as a function of temperature.

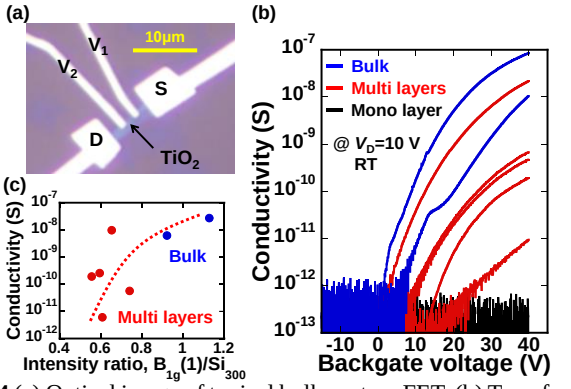

Fig. 4 (a) Optical image of typical bulk anatase FET. (b) Transfer characteristics. (c) Conductivity as a function of $B_{1g}(1)/Si_{300}$.

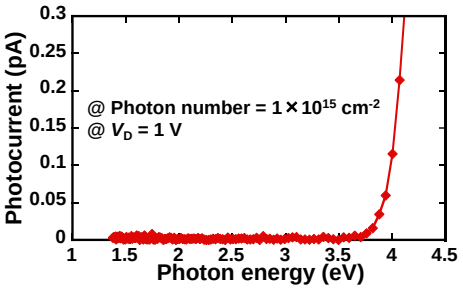

Fig. 5 Photocurrent spectra measured for bulk anatase FET without back gate bias.

monolayer samples are polycrystalline and amorphous, respectively.

Figure 4(a) shows an optical image of typical anatase FET fabricated by conventional electron beam lithography technique. The source and drain electrodes are Al. **Figure 4(b)** is the transfer characteristics for anatase FETs measured at room temperature in vacuum of ~10^{-2} Pa. No current modulation is observed for monolayer, while multilayer and bulk with the thickness of 8~15 nm exhibit the clear transistor operation. As shown in **Fig. 4(c)**, There is clear relationship between conductivity at V_G - V_{th} = 5 V and $B_{1g}(1)/Si_{300}$ intensity ratio, indicating that the current modulation strongly depends on the crystallinity. The best values for field effect mobility analyzed by 4 probe measurement and current on/off ratio is 0.23 cm^2/Vs and ~10^6, respectively. There values are comparable with those in the previous reports. It should be noted that the current modulation of anatase TiO_2 FET thinner than 10 nm is achieved in this study.

3. Characterization of in-gap states

Photocurrent measurement often provides the information of defects in a band gap. Indeed, the previous report on anatase fabricated by the pulsed laser deposition clearly show the peak around 2 eV associated with the oxygen vacancies [5]. **Figure 5** shows photocurrent spectrum of bulk anatase FET sample measured in the off-state as a function of photon energy. It is evident that in-gap states are negligible. Because of single crystalline nature, the defects related with oxygen vacancies may be quite limited, compared with the grain boundaries in the deposited film. Moreover, photocurrent edge, which reflects bandgap, shifts from 3.2 eV of the typical anatase to 3.8 eV of the present bulk anatase. If the present bulk sample includes both anatase and $Ti_{0.87}O_2$ nanosheet (E_G = 3.8 eV), the lower energy edge of 3.2 eV should be observed as a shoulder. However, this is not the case, since Raman and EBSP analysis clearly indicates the solid state transformation from nanosheet to anatase. Interestingly, the detailed analysis on Raman $E_g(1)$ show the red shift of $E_g(1)$ by ~3 cm^{-1} from the typical anatase, suggesting the existence of the lattice distortion. This may be the reason for larger energy gap. Based on these discussion, the present anatase seems to be different from that fabricated by conventional deposition methods, which provides new opportunity to study catalytic property induced by electric field effect.

4. Conclusions

The anatase FETs with the channel thickness less than 10 nm was successfully fabricated through the solid-state transformation from $Ti_{0.87}O_2$ nanosheet. We demonstrate the reasonably high mobility of 0.23 cm^2/Vs and high on/off current ratio of 10^6. This may provide the future application to control the catalytic property by electric field effect.

References

[1] G. Oike, *et al.*, *IEDM Tech. Dig*. 2013, 300.
[2] M. Katayama, *et al.*, *APL*. 2006, 89, 242103.
[3] J.-W. Park, *et al.*, *IEEE EDL*, 2009, 30, 362.
[4] M. Osada *et al.*, *Adv. Mater*. 2012, 24, 210-228.
[5] T. Yajima *et al.*, Phys. Status Solidi A 2016, (in press).